forests

MDPI

Article

Preparation and Properties of Soft-/Hard-Switchable Transparent Wood with 0 °C as a Boundary

Yang Liu [1], Yi Zhang [1], Jianhui Guo [1,*], Gaiping Guo [2,3] and Cheng Li [4,*]

[1] Department of Environmental Design, College of Fine Arts, Henan University, Kaifeng 475001, China
[2] Department of Chemical Engineering, Tsinghua University, Beijing 100084, China
[3] College of New Materials and Chemical Engineering, Beijing Institute of Petrochemical Technology, Beijing 102617, China
[4] College of Forestry, Henan Agricultural University, Zhengzhou 450002, China
* Correspondence: gjh1985@henu.edu.cn (J.G.); lichengzzm@163.com (C.L.)

Abstract: Transparent wood has excellent optical and thermal properties and has great potential utilization value in energy-saving building materials, optoelectronic devices, and decorative materials. In this work, transparent wood with soft-/hard-switchable and shape recovery capabilities was prepared by introducing an epoxy-based polymer with a glass transition temperature of about 0 °C into the delignified wood template. The epoxy resin was well filled in the pore structure of the delignified wood, and the as-prepared wood exhibited excellent transparency; the optical transmittance and haze of the transparent wood with a thickness of 2.0 mm were approximately 70% and 95%, respectively. Because the glass transition temperature of the epoxy-based polymer was about 0 °C, the prepared transparent wood was rigid below 0 °C and flexible above °C; meanwhile, the transparent wood exhibited shape change and shape recovery properties. Incorporating optical transparency and soft-/hard-switchable ability into the transparent wood opens a new avenue for developing advanced functional wood-based materials.

Keywords: transparent wood; epoxy polymer; optical properties; flexibility; shape change

Citation: Liu, Y.; Zhang, Y.; Guo, J.; Guo, G.; Li, C. Preparation and Properties of Soft-/Hard-Switchable Transparent Wood with 0 °C as a Boundary. *Forests* **2024**, *15*, 384. https://doi.org/10.3390/f15020384

Academic Editors: Zeki Candan and Mehmet Hakki Alma

Received: 8 December 2023
Revised: 6 February 2024
Accepted: 13 February 2024
Published: 19 February 2024

1. Introduction

As a natural biomass material, wood has excellent properties such as a high ratio of strength to weight, low thermal conductivity, non-toxicity, and degradability [1]. The unique structure formed during its natural growth gives it excellent mechanical properties, making it a good structural material, and it is widely used in structural architecture, interior decoration and furniture, wood art products, and many other aspects. Wood is easily degradable, renewable, and non-polluting, making it one of the most readily available green materials [2]. It can replace some non-renewable resources, which aligns with the concept of sustainable development in today's era. However, due to its inherent structure and chemical composition, wood is opaque [3], which, to a certain extent, hinders the application of wood in the optical field [4,5].

In recent years, as a new type of wood-layered structural material [6], transparent wood has great environmental and economic benefits [7], which not only retains most of the natural properties of wood but also gives it excellent optical and mechanical properties [8,9]. Its excellent properties, such as strong mechanical properties [10], low density, good thermal insulation [11], transparency, and green environmental protection, have attracted wide attention, and it has broad application prospects in many aspects, such as intelligent, transparent buildings [12,13], furniture materials, thermal energy storage, and electronic devices [14,15]. On the one hand, delignification can remove the colored structural groups in the wood lignin, and on the other hand, it can increase the porosity of the wood, thus providing more penetration paths for the subsequent impregnation of the polymer [16]. Transparent wood is usually made of wood as a matrix, through delignification or partial

removal of lignin and hemicellulose to obtain a delignified wood template, and then impregnated with a resin matching the refraction coefficient of delignified wood to prepare it [17,18]. Therefore, the resin type largely determines the properties of transparent wood.

The resin impregnation process used for the preparation of transparent wood requires, on the one hand, that the selected resin must match the refraction coefficient of the delignified wood template [19], and on the other hand, the viscosity of the resin also needs to be appropriate, meaning it is easier to penetrate the pore structure of the delignified wood [20]. Resin impregnation modification can process wood into a new bio-based material with great potential, which can not only retain the natural characteristics of wood, such as easy processing and good mechanical properties, but also improve its natural defects, such as easy deformation, poor dimensional stability, and poor corrosion resistance [21]. The selected resins mainly include epoxy resin, methyl methacrylate (MMA), polyvinyl alcohol (PVA), etc. Li et al. [22] selected MMA as the filling resin, impregnated delignification wood, and prepared transparent wood with a thickness of 1.2 mm, light transmit rate of 85%, and fog degree of 71% after curing. Anantha et al. [17] produced transparent wood with high light transmissivity, fog degree, and flexibility by regulating the content of propylene glycol used as a plasticizer in polyvinyl alcohol PVA. At the same time, Anantha et al. [23] also introduced the poplar veneer with PVA to produce biodegradable and highly elastic transparent wood. Yang et al. [24] obtained transparent wood with excellent stretchability (maximum tensile strain up to 73.9%) and good temperature sensitivity through photo-induced polymerization, which infiltrated deep eutectic solvents into the delignified wood template. Cai et al. [25] and Tan et al. [26] exploited the properties of epoxy-based polymers to enhance optical and mechanical properties, directional scattering effects, and unique shape management capabilities of delignified wood, thereby expanding the application of transparent wood.

Nanoparticles have attracted much attention in composite materials because they can provide structural color, magnetism, optics, and other functions [27,28]. Various nanoparticles are added to the polymer and then impregnated into the delignified wood to obtain transparent wood with excellent mechanical and optical properties [29,30], and some also have near-infrared thermal shielding and ultraviolet shielding functions [31], which can improve their thermal insulation and can be a potential substitute for energy-saving building materials such as smart windows. Wu et al. [32] uniformly dispersed TiO_2 nanoparticles into epoxy resin polymers and filled them into a delignified frame to obtain dual-function transparent wood with UV shielding and heat insulation properties, with a transmission rate of 90% and a thermal conductivity of only 0.3228 W/mK, which can be used as an alternative material for green energy-saving heat insulation windows. Aldalbahi et al. [33] mixed MMA, ammonium poly-phosphate (APP), and lanthanide-doped strontium aluminate (LSA) phosphor nanoparticles in a certain proportion, which underwent ultrasonic to uniform dispersion, and vacuum permeated the solution into the lignin-modified linden wood substrate. A type of long-term luminous, transparent wood with flame retardant, UV shielding, and super hydrophobic properties was obtained. Rahayu et al. [34] impregnated Jabon (*Anthocephalus cadamba*) with iron solution and soaked it in strong or weak alkali. Magnetite (Fe_3O_4) was formed in the wood, and a supermagnetic material with soft magnetic properties was prepared. In addition, transparent wood is also involved in advanced fields such as thermal insulation and energy-saving wood windows, wood bionic seawater evaporators, radiation cooling energy-saving buildings, and so on [35]. Therefore, research on transparent wood and tapping into its multi-functional potential has become a hot topic.

Although the preparation of transparent wood using a variety of resins and functional nanoparticles doped in resins has been widely reported, soft-/hard-switchable transparent wood with 0 °C as a boundary has not been reported. In this work, the soft-/hard-switchable transparent wood was prepared in two steps. Firstly, the wood was delignified by a mixture solution of sodium chlorite and glacial acetic acid to obtain a delignified wood template. Secondly, the transparent wood with soft-/hard-switchable and shape recovery

capabilities was prepared by introducing the epoxy-based polymer with a glass transition temperature of about 0 °C into the delignified wood template. The as-prepared wood exhibited excellent optical transparency and shape switchability. The transparent wood's microstructure, chemical composition, optical properties, mechanical properties, and shape changes were characterized.

2. Materials and Methods

2.1. Materials and Chemicals

Balsa wood (*O. pyramidale*) with a density of about 105 ± 3.6 mg/cm^3 was purchased from Zhuhai Dechi Technology Co., Ltd., Zhuhai, China. Sodium chlorite ($NaClO_2$, 80%) and glacial acetic acid (CH_3COOH, 99.5%) were purchased from Shanghai Aladdin Reagent Co., Ltd., Shanghai, China). Trimethylol propane tri (3-mercaptopropionic acid) ester (90%) and stannous caprylate ($Sn(Oct)_2$, 95%) were purchased from Shanghai Maclin Biochemical Technology Co., Ltd., Shanghai, China. The IN_2 Epoxy conductive resin (ECR) was purchased from a store (Taobao) that sold the Easycomposites brand. All solvents were used without further purification.

2.2. Preparation of Delignified Wood Formwork

Natural balsa wood was cut into slices (cross-section) with the dimensions 40 mm × 40 mm × 2 mm. Next, 1 wt % $NaClO_2$ solution was prepared and the pH was adjusted to 8.5 with glacial acetic acid. The wood chips were immersed in the delignification solution at 80 °C for 18 h, changing the delignification solution every 6 h until they were completely white. The wood chips were thoroughly rinsed with deionized water at 80 °C to remove excess chemicals and then vacuum-dried in a freeze-dryer to obtain a delignified wood template. The sample size was 40 mm × 5 mm × 2 mm, and the tensile speed was 5 mm/min. The test was repeated three times.

2.3. Preparation of Transparent Wood

Firstly, the epoxy polymer impregnation solution was prepared: a certain proportion of ECR and trimethylolpropane tri (3-mercaptopropionic acid) ester were added to the beaker, and then the catalyst strenuous $Sn(Oct)_2$ was added to the above-mixed solution (the catalyst was 5% of the mole fraction of the sulfhydryl group) and was vigorously stirred. The delignified wood was placed in the bottom of the epoxy polymer impregnation solution, and the vacuum impregnation time was about 20 min at room temperature. After that, the delignified wood chips impregnated with the epoxy polymer were taken out and placed between two polytetrafluoron films and cured at 120 °C for 2 h.

2.4. Characterization and Testing

The glass transition temperature was detected. A differential scanning calorimeter (TA DSC, 250, New Castle, DE, USA) was used to test the glass transition temperature of the sample. The test temperature range was −80 °C to 200 °C, and the heating rate was 10 °C/min in a nitrogen atmosphere. The wood samples were pretreated by slicing and then glued to the stage with conductive adhesive. After gold spraying and vacuum extraction, the morphology and microstructure of the wood surface and cross-section microstructure were observed by scanning electron microscopy (SEM) (Hitachi Regulus 8100). The acceleration voltage was 5.0 kV. The samples were ground into powder and sieved through a 200-mesh sieve for subsequent analysis. Fourier Transform Infrared Spectroscopy (FTIR) utilizing Attenuated Total Reflection (ATR) was employed to characterize the structural composition of the wood samples. Specifically, a Nicolet Instrument Corporation 6700 spectrometer (Madison, WI, USA) was utilized, employing parameters of 32 scans and a resolution of 4 cm^{-1} within the spectral range of 4000–600 cm^{-1}. The chemical composition of the treated wood was assessed using a chemical composition tester (F800, Hanon Future Technology Group Co., Ltd., Shanghai, China). The relative proportions of cellulose, hemicellulose and lignin within the samples were determined via the Van Soest

method. Optical performance was assessed via the light transmittance, fog degree and light scattering tests. The light transmittance and fog degree of transparent wood were tested by a fog meter (Diffusion EEL 57D fog meter in the UK with an integrating sphere) with a visible light wavelength of 400–800 nm. The light scattering experiment on transparent wood adopted the acquisition system made by the laboratory, which mainly includes a laser and laser illuminometer and other laser generation and intensity acquisition components. A universal mechanical testing machine (SHIMADZU AGS-X10KN, Kyoto, Japan) was used to test the tensile strength of wood samples. The sample size was 40 mm × 5 mm × 2 mm, and the tensile speed was 5 mm/min. All the characterization tests were repeated three times, where applicable.

2.5. Shape Deformation Behaviors

The size of the transparent wood was 40 mm × 5 mm × 2 mm. At different temperatures, pressure was applied to one end of the transparent wood to record its bending degree. The prepared transparent wood was bent into different shapes at a certain temperature and then placed without applying external forces to record its shape recovery ability. The shape-memory capability of the TW was quantitatively characterized using a bending deformation mode. The transparent wood strips were gently folded in the middle at 30 °C and immersed in 0 °C water for fixation. The bending angles at specific times were calculated using the digital photographs recorded at different temperatures during the shape transformation process.

3. Results and Discussion

3.1. Glass Transition Temperature and Mechanical Properties of Transparent Wood

Figure 1 shows the schematic diagram of the reaction mechanism of the epoxy resin polymer. The epoxy resin monomer used is an epoxy conductive resin, which has a low viscosity and is convenient for later impregnation into the pore structure of delignified wood. The epoxy group of the conductive resin and the sulfhydryl group of the sulfhydryl compound produce a three-dimensional cross-linked network structure under the action of the catalyst stannous caprylate. The polymer produced by the reaction shows a transparent state.

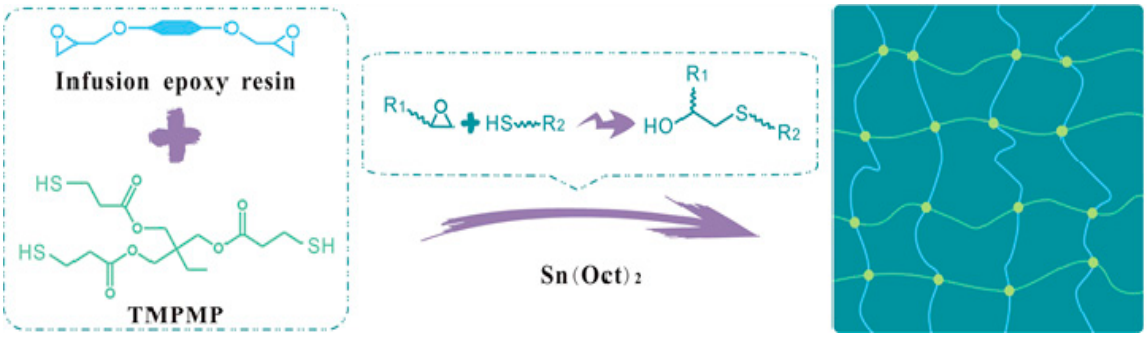

Figure 1. The reaction process of epoxy resin polymer.

The glass transition temperature of the prepared epoxy resin polymer is shown in Figure 2. The Tg of the prepared epoxy resin polymer is about 0 °C, indicating that it is lower than 0 °C, the polymer is glassy, the molecular structure is a stable three-dimensional cross-linked network, and the polymer has a certain strength and hardness. When the temperature is higher than 0 °C, the molecular chain of the polymer moves, and the macro performance is polymer softening. At room temperature (25 °C), the polymer is flexible. Therefore, this polymer is impregnated into the pores of the wood delignification template, and the prepared transparent wood is theoretically flexible transparent wood.

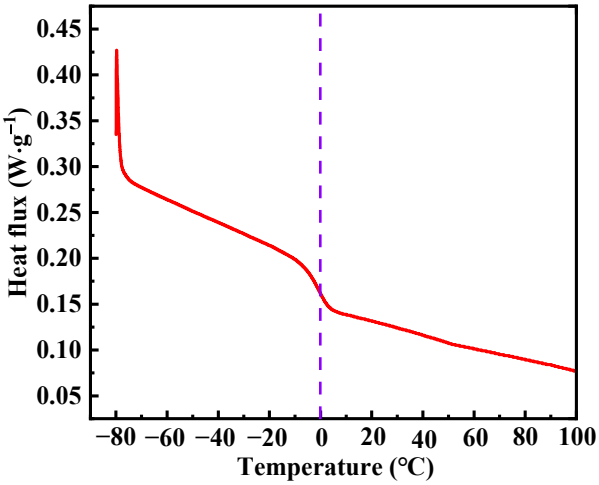

Figure 2. DSC curve of epoxy resin polymer.

A universal mechanical testing machine (SHIMADZU AGS-X10KN, Kyoto, Japan) was used to test the tensile strength of wood samples. (strain: the ratio of the stretching distance to the length of the original sample). The original length of transparent wood used for mechanical tensile testing was 40 mm. Figure 3 shows the tensile strength of the prepared epoxy polymer at room temperature (25 °C). The polymer is flexible at room temperature, and it can be seen from the stress–strain curve that the tensile fracture strength of the prepared polymer is about 2.6 MPa, and the elongation at break is about 98.6%. Therefore, the polymer has a certain flexibility at room temperature.

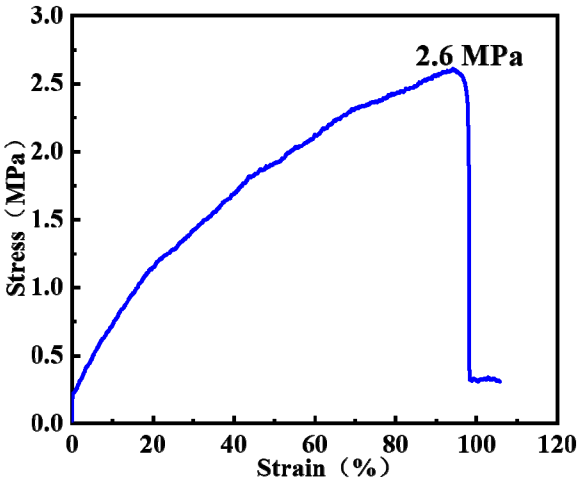

Figure 3. Stress–strain curve of epoxy resin polymer.

3.2. Microstructure of Transparent Wood

The preparation process of transparent wood is shown in Figure 4. The wood used in this experiment is the balsa wood cross-section, the size of which is 40 mm × 40 mm × 2 mm. First, it can be seen that the original balsa wood chip is the light yellow color of the wood itself and is opaque. After the delignification treatment, the wood chip appears white, and the text on the bottom can be seen faintly through the delignification wood chip. When it was further impregnated with the epoxy polymer, it was observed that the wood/polymer composite presented a transparent state and the writing on the bottom could be clearly seen.

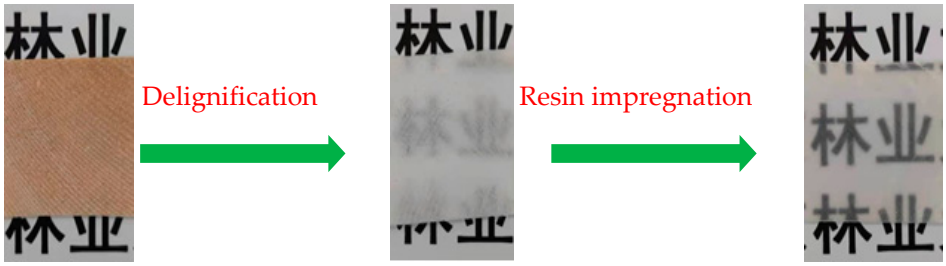

Figure 4. Schematic diagram of the preparation process of transparent wood.

$NaClO_2/CH_3COOH$ acid delignification solution was used to delignify wood. As can be seen from Figure 5a, the contents of cellulose, hemicellulose, and lignin in natural balsa wood were 48.3%, 25.6%, and 26.1%, respectively. After delignification, the relative contents of cellulose, hemicellulose and lignin were 76.2%, 18.4% and 5.4%, respectively. The content of hemicellulose and lignin decreased, obviously due to delignification, resulting in the relative content of cellulose increasing by 57.8%. Wood is composed of three main components: cellulose, hemicellulose and lignin. The delignification process partially removes hemicellulose and lignin components, leading to a decrease in the density of delignified wood. However, after impregnation with epoxy resin and curing, the density of transparent wood significantly increases. We calculated the apparent density of natural balsa wood, delignification wood, ECR, and transparent wood (Figure 5b). The results showed that after delignification, the apparent density of natural balsa wood decreased from 0.105 g/cm^3 to 0.065 g/cm^3. After epoxy polymer impregnation, the density of transparent wood increased to 1.032 g/cm^3. The mass of epoxy polymer accounts for 93.7% of the total mass of transparent wood.

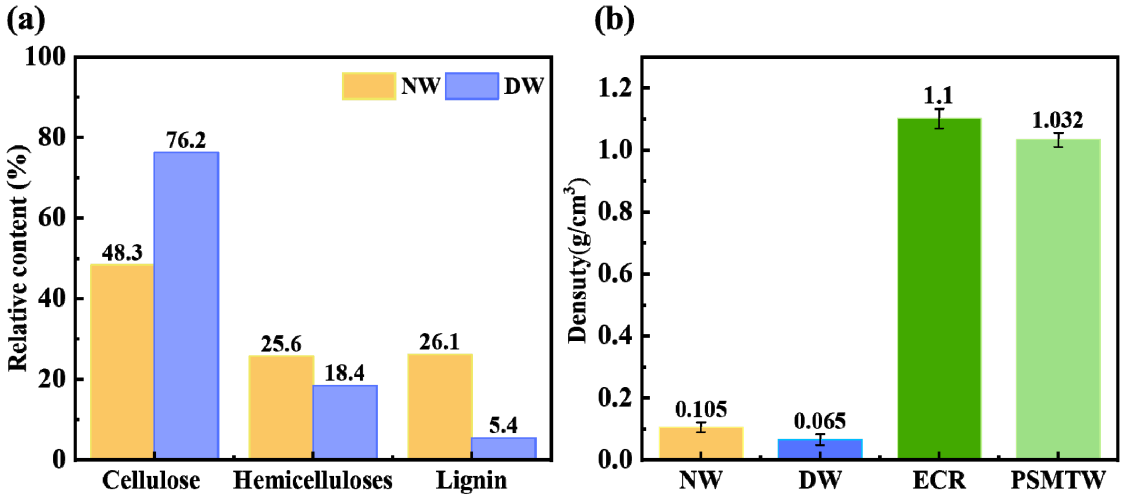

Figure 5. (**a**) The three major wood elements (the relative content of cellulose, hemicellulose, and lignin) before and after delignification; (**b**) the apparent density of raw, delignified, ECR, and transparent wood.

SEM images of the cross-sectional microstructure of natural wood, delignified wood and transparent wood are shown in Figure 6. Natural balsa wood has a unique three-dimensional layered and interconnected honeycomb porous structure (shown in Figure 6a,a$_1$), showing a high degree of anisotropy, and its porous structure is conducive to polymer infiltration and filling into the wood micropores. However, as can be seen from the picture, the vessel cell wall in the wood is thicker, the cells are closely connected, and the cell space is less. After delignification treatment, the overall micro-morphological structure of the wood remained unchanged (Figure 6b). Compared with natural balsa wood, the structure of delignified wood is looser and the cell wall is thinner (Figure 6b$_1$).

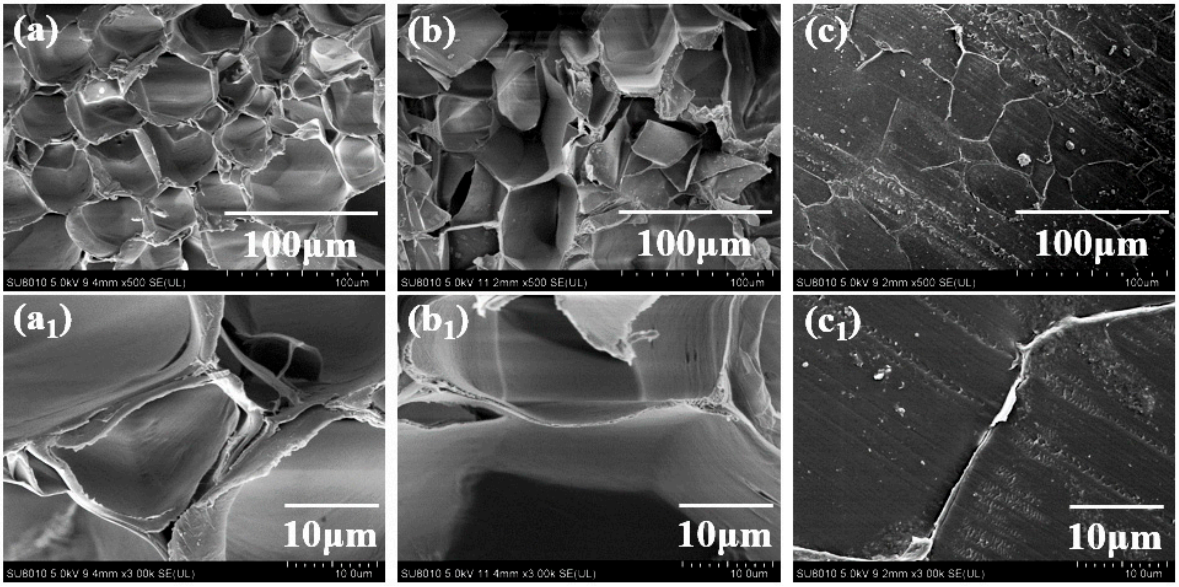

Figure 6. The microstructure of raw wood, delignified wood, and transparent wood. (**a**,**a$_1$**) SEM pictures of the cross-section of the original wood; (**b**,**b$_1$**) SEM pictures of the cross-section of the delignified wood; (**c**,**c$_1$**) SEM pictures of the cross-section of transparent wood.

The scanning electron microscope image of transparent wood (Figure 6c,c$_1$), after impregnation with the epoxy polymer, shows that the cross section of transparent wood has changed significantly compared with delignified wood. After infiltration filling, the micro-porous structure of the wood remains unchanged. The polymer is uniformly filled into the wood cell cavity, forming a smooth film on the micro-morphology of the cross section of transparent wood. The combination with the cell wall is relatively close, which can effectively reduce light scattering and improve light transmittance. The increase in the relative content of cellulose in delignified wood increases the strong interaction between cellulose and the impregnated polymer due to hydrogen bonding or van der Waals force [36].

3.3. Characterization of Chemical Constituents of Transparent Wood

The chemical composition changes in the epoxy monomer compound and sulfhydryl monomer compound to produce the pure resin polymer are shown in Figure 7a. The characteristic peaks of the sulfhydryl group (2567 cm^{-1}) and the epoxy conductivity resin (910 cm^{-1}) disappear in the pure polymer system, and the signal peaks of the hydroxyl group appear at 3200–3600 cm^{-1}. This shows that the epoxy group of the epoxy conductive resin reacts with the sulfhydryl group in trimethylolpropane III (3-mercaptopropionic acid) ester, and a large number of hydroxyl groups are formed at the same time. The changes in these characteristic peaks are consistent with the reaction mechanism of the epoxy polymer in Figure 1. The cell wall components of wood are composed of cellulose, hemicellulose, lignin, etc. After the delignification of raw wood, the characteristic peaks of lignin at 1595 cm^{-1} and 1504 cm^{-1} disappear (Figure 7b), indicating that after the delignification of raw wood, a large number of lignin components are removed. It is worth noting that, due to the relatively low mass ratio of the delignified wood template in the transparent wood (only 6.3% of the mass fraction of the transparent wood), the transparent wood shows an infrared profile similar to that of the pure polymer.

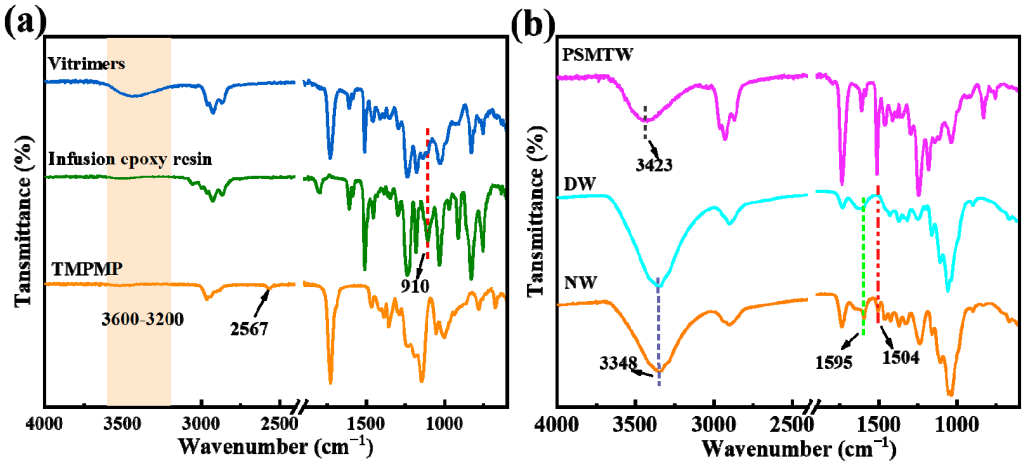

Figure 7. (**a**) Infrared spectra of infusion resin, trimethylolpropane tris(3-mercaptopropionate), and pure polymer; (**b**) infrared spectra of raw, delignified, and transparent wood.

3.4. Optical Properties of Transparent Wood

Optical transparency is one of the most important characteristics of transparent wood. Figure 8a shows the prepared transparent wood's light transmittance and fog degree in the visible range (400–800 nm). The thickness of the transparent wood was about 2 mm. The results showed that the light transmittance of the transparent wood was about 70%, and the fog degree was higher than 95%. Its transparency was lower than many reported transparent woods, but its haze was higher than most transparent woods, as shown in Table 1 (only relevant data for some reported transparent woods). As shown in Figure 8b, the laser beam passed through the transparent wood (cross-section plane), leaving an isotropic light spot distribution on the back bottom. We tested the intensity distribution of the scattered light on the X and Y axes, and the results showed that the scattered light was evenly distributed along the X and Y axes, conforming to the Gaussian distribution (normal distribution). A green laser beam (532 nm) was passed perpendicularly through the transparent wood sample, which showed Gaussian light scattering performance due to the directional arrangement of wood fibers. This Gaussian light scattering behavior was caused by the refractive index fluctuations due to the aligned fibers.

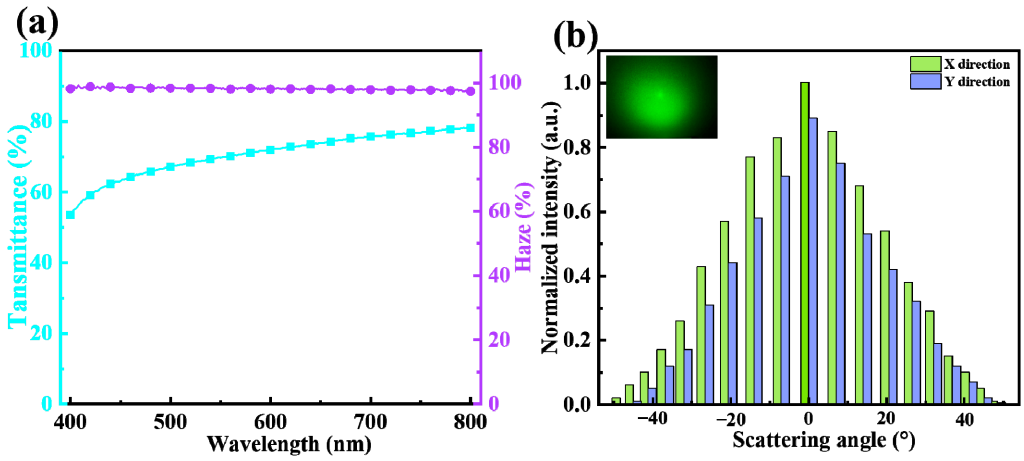

Figure 8. Optical properties of transparent wood. (**a**) The light transmittance and haze of transparent wood; (**b**) the light scattering distribution of the cross-section of transparent wood along the X-axis and Y-axis.

3.5. Mechanical Properties of Transparent Wood

Figure 9 shows the stress–strain curves (transverse) of raw wood, delignified wood, and clear wood at room temperature. The radial × chord × longitudinal dimensions of transparent wood specimens are 40 mm × 40 mm × 2 mm. The experimental sample was small wood chips in the transverse section of the wood with not much difference in their tangential and radial strength. The tensile strength of the original wood was about 0.49 MPa, which decreased significantly to 0.09 MPa after delignification. However, the tensile strength of the transparent wood filled with the epoxy polymer was about 1.44 MPa. Because the pure polymer is flexible at room temperature, the elongation at break of transparent wood was greater than 20%, which was much higher than that of raw wood and delignified wood.

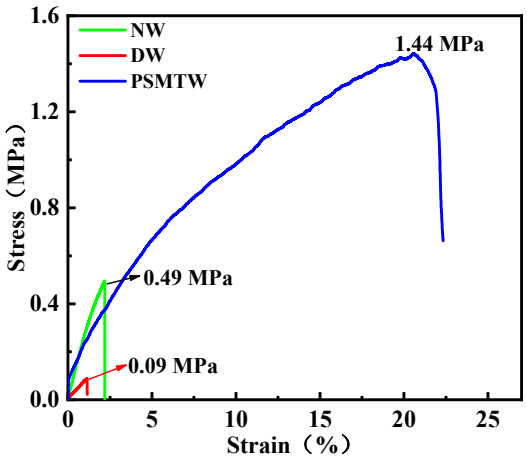

Figure 9. Stress–strain curve of the original wood, delignified wood, and transparent wood.

The occurrence of light scattering mainly occurs at the interface between cellulose and polymers. Light scattering is uniformly distributed in the fiber direction and exhibits anisotropy in the vertical fiber direction [37]. The removal of lignin will inevitably lead to a decline in the mechanical properties of wood since it is a crusting material that hardens and penetrates between the woody cell wall skeleton materials (cellulose). After filling with the epoxy polymer, the mechanical tensile properties of the prepared transparent wood were significantly improved. However, the tensile break strength and elongation at break of the transparent wood were lower than those of the pure epoxy polymer samples (tensile break strength and elongation at break were about 2.6 MPa and 98.6%). This could be because the delignified wood's conduit cells in the transparent wood interrupted the continuity of the pure polymer to a certain extent, resulting in the reduction in mechanical properties. Compared with the tensile strength of other transparent wood in literature, it needs to be improved, as shown in Table 1.

3.6. Flexibility of Transparent Wood

It can be seen from the epoxy polymer's DSC curve that the polymer's Tg is about 0 °C. When the temperature is lower than 0 °C, the polymer is a stable three-dimensional cross-linked network without molecular chain movement and demonstrates rigidity. When the temperature is higher than 0 °C, the molecular chain in the polymer system moves, and the polymer is flexible. Therefore, when the polymer is introduced into the delignification wood system, the prepared transparent wood will also show rigid or flexible states at temperatures below or above Tg. As shown in Figure 10, the left figure shows that the transparent wood maintains a flat state under the stress at −20 °C. When the temperature is at room temperature (25 °C), a certain degree of bending of transparent wood can be observed when the end is stressed. This indicates that transparent wood exhibits rigid or flexible characteristics when the ambient temperature is lower than or higher than Tg.

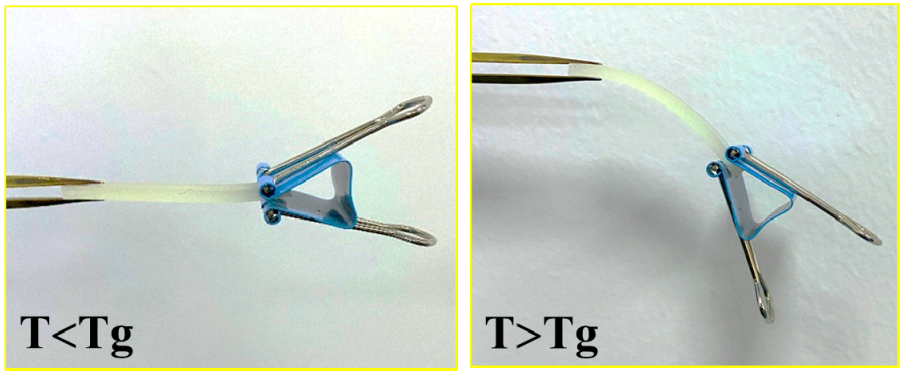

Figure 10. Stiffness and flexibility of transparent wood when the temperature is higher than or lower than Tg.

Figure 11 shows a diagram of the flexibility and shape recovery ability of the transparent wood. At room temperature, the transparent wood was flexible and could be shaped into any form. After forming a "U"- and "S"-shape of the transparent wood and placed in an environment where the temperature was lower than Tg, the shapes were fixed. However, when the transparent wood was placed at room temperature again, it gradually regained its original long shape. This is because at temperatures higher than Tg, the molecular chain of the polymer in the transparent wood will move due to the increase in entropy and since the polymer occupies a large proportion of the transparent wood, the transparent wood will then regain its original shape. As can be seen in Table 1, the light transmittance of the transparent wood in this study was better compared with the optical and mechanical properties of other transparent wood in literature, but there is still room for improvement, along with its low tensile strength. Moreover, its high haze is conducive to privacy security if used as material for windows.

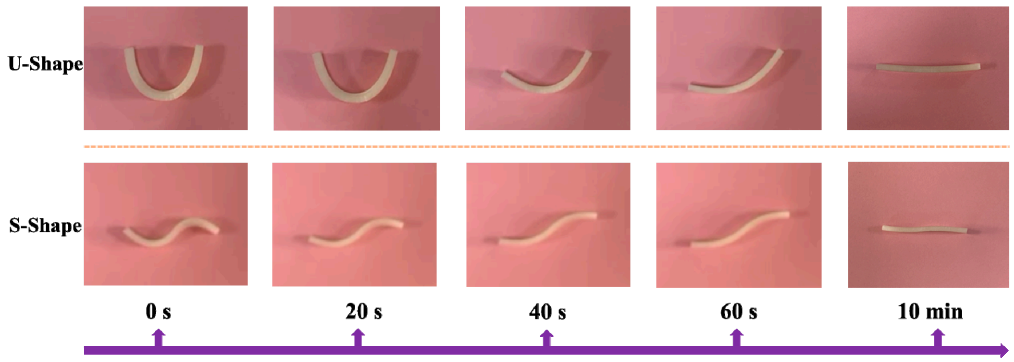

Figure 11. Flexibility and shape-recovery capability of transparent wood.

Table 1. Comparison of optical and mechanical properties of different transparent wood.

Materials	Transmittance (%)	Haze (%)	Ultimate Tensile Strength (MPa)	Ref.
Lignin-retaining transparent wood	83	75	-	[12]
Transparent compressed wood	90	70	113.75	[18]
Thermochromic wood	50.5	70	130.6	[38]
Transparent wood	81.07	-	59.92	[39]
Soft-/hard-switchable transparent wood	70	>95	1.44	This work

4. Conclusions

(1) An epoxy polymer with a low glass transition temperature was prepared and used for impregnating a delignified wood template to form transparent wood with low-temperature rigidity and high-temperature flexibility.

(2) Compared with original wood, transparent wood exhibited improved tensile strength and elongation at break at room temperature, good transparency, and excellent haze. The glass transition temperature of epoxy polymers is about 0 °C, resulting in the prepared transparent wood being rigid at low temperatures (T < Tg) and flexible at high temperatures (T > Tg). This allows the prepared transparent wood to be used to make multi-shaped transparent wood windows and wood decorations.

(3) The prepared transparent wood exhibited excellent optical properties but with low tensile strength and tensile fracture strength. Therefore, it is necessary to develop strategies to strengthen the optical and mechanical properties of the transparent wood in future research.

Author Contributions: Conceptualization, J.G. and Y.L.; methodology, Y.L., J.G. and C.L.; validation, G.G. and Y.Z.; formal analysis, Y.L. and J.G.; investigation, Y.L., C.L., J.G. and Y.Z.; resources, J.G.; data curation, G.G. and Y.Z.; writing—original draft preparation, Y.L., J.G. and C.L.; writing—review and editing, J.G. and Y.L.; visualization, J.G.; supervision, C.L. and J.G.; project administration, Y.L. and J.G.; funding acquisition, Y.L. All authors have read and agreed to the published version of the manuscript.

Funding: This work was supported by the Philosophy and Social Science Planning Program of Henan Province (Grant No.2020BYS004), and the Special Project on Cultural Research for the Revitalization of Culture Project in Henan Province (2023XWH130).

Data Availability Statement: The data presented in this study are available upon request from the corresponding author.

Conflicts of Interest: The authors declare no conflicts of interest.

References

1. Luan, Y.; Fang, C.-H.; Ma, Y.-F.; Fei, B.-H. Wood mechanical densification: A review on processing. *Mater. Manuf. Process.* **2022**, *37*, 359–371. [CrossRef]
2. Zhang, H.; Wang, X.; Wang, Y.; Gu, Z.; Chen, L. Bi-functional water-purification materials derived from natural wood modified TiO_2 by photothermal effect and photocatalysis. *RSC Adv.* **2022**, *12*, 26245–26250. [CrossRef]
3. Mariani, A.; Malucelli, G. Transparent wood-based materials: Current state-of-the-art and future perspectives. *Materials* **2022**, *15*, 9069. [CrossRef]
4. Dong, Y.; Wang, J.; Wang, K.; Li, C.; Cai, Y.; Li, J.; Lam, S.S.; Sonne, C. High-performance and scalable wood-based solar-driven interfacial evaporator with corrugated structure for continuous desalination. *J. Clean. Prod.* **2023**, *418*, 138024. [CrossRef]
5. Wang, Y.; Sun, G.; Dai, J.; Chen, G.; Morgenstern, J.; Wang, Y.; Kang, S.; Zhu, M.; Das, S.; Cui, L.; et al. A high-performance, low-tortuosity wood-carbon monolith reactor. *Adv. Mater.* **2017**, *29*, 1604257. [CrossRef]
6. Yang, H.; Wang, H.; Cai, T.; Ge-Zhang, S.; Mu, H. Light and wood: A review of optically transparent wood for architectural applications. *Ind. Crops Prod.* **2023**, *204*, 117287. [CrossRef]
7. Wan, C.; Liu, X.; Huang, Q.; Cheng, W.; Su, J.; Wu, Y. A brief review of transparent wood: Synthetic strategy, functionalization and ap-plications. *Curr. Org. Synth.* **2021**, *18*, 615–623. [CrossRef]
8. Hu, Y.; Zhang, Y.; Cai, W.; Ming, Y.; Yu, R.; Yang, H.; Noor, N.; Fei, B. Transparent wood with heat shielding and high fire safety properties for energy saving applications. *Renew. Energ.* **2023**, *219*, 119426. [CrossRef]
9. Zhu, M.; Li, T.; Davis, C.S.; Yao, Y.; Dai, J.; Wang, Y.; AlQatari, F.; Gilman, J.W.; Hu, L. Transparent and haze wood composites for highly efficient broadband light management in solar cells. *Nano Energy* **2016**, *26*, 332–339. [CrossRef]
10. Fu, Q.; Yan, M.; Jungstedt, E.; Yang, X.; Li, Y.; Berglund, L.A. Transparent plywood as a load-bearing and luminescent biocomposite. *Compos. Sci. Technol.* **2018**, *164*, 296–303. [CrossRef]
11. Dong, Y.; Tan, Y.; Wang, K.; Cai, Y.; Li, J.; Sonne, C.; Li, C. Reviewing wood-based solar-driven interfacial evaporators for desalination. *Water Res.* **2022**, *223*, 119011. [CrossRef]
12. Li, Y.; Fu, Q.; Rojas, R.; Yan, M.; Lawoko, M.; Berglund, L. Lignin-retaining transparent wood. *ChemSusChem* **2017**, *10*, 3445–3451. [CrossRef]
13. Yaddanapudi, H.S.; Hickerson, N.; Saini, S.; Tiwari, A. Fabrication and characterization of transparent wood for next generation smart building applications. *Vacuum* **2017**, *146*, 649–654. [CrossRef]

14. Li, Y.; Vasileva, E.; Sychugov, I.; Popov, S.; Berglund, L. Optically transparent wood: Recent progress, opportunities, and challenges. *Adv. Opt. Mater.* **2018**, *6*, 1800059. [CrossRef]
15. Wang, L.; Liu, Y.; Zhan, X.; Luo, D.; Sun, X. Photochromic transparent wood for photo-switchable smart window applications. *J. Mater. Chem. C* **2019**, *7*, 8649–8654. [CrossRef]
16. Tang, Q.; Fang, L.; Wang, Y.; Zou, M.; Guo, W. Anisotropic flexible transparent films from remaining wood microstructures for screen protection and agnw conductive substrate. *Nanoscale* **2018**, *10*, 4344–4353. [CrossRef]
17. Rao, A.N.S.; Nagarajappa, G.B.; Nair, S.; Chathoth, A.M.; Pandey, K.K. Flexible transparent wood prepared from poplar veneer and polyvinyl alcohol. *Compos. Sci. Technol.* **2019**, *182*, 107719.
18. Wang, Y.; Wu, Y.; Yang, F.; Yang, L.; Wang, J.; Zhou, J.; Wang, J. A highly transparent compressed wood prepared by cell wall densification. *Wood Sci. Technol.* **2022**, *56*, 669–686. [CrossRef]
19. Fink, S. Transparent wood—A new approach in the functional study of wood structure. *Holzforschung* **1992**, *46*, 403–408. [CrossRef]
20. Wu, Y.; Zhou, J.; Huang, Q.; Yang, F.; Wang, Y.; Wang, J. Study on the properties of partially transparent wood under different delignification processes. *Polymers* **2020**, *12*, 661. [CrossRef]
21. Spear, M.J.; Curling, S.F.; Dimitriou, A.; Ormondroyd, G.A. Review of functional treatments for modified wood. *Coatings* **2021**, *11*, 327. [CrossRef]
22. Li, Y.; Fu, Q.; Yu, S.; Yan, M.; Berglund, L. Optically transparent wood from a nanoporous cellulosic template: Combining functional and structural performance. *Biomacromolecules* **2016**, *17*, 1358–1364. [CrossRef]
23. Wang, J.; Zhu, J. Prospects and applications of biomass-based transparent wood: An architectural glass perspective. *Front. Chem.* **2021**, *9*, 747385. [CrossRef]
24. Yang, L.; Wu, Y.; Yang, F.; Wang, W. Study on the preparation process and performance of a conductive, flexible, and transparent wood. *J. Mater. Res. Technol.* **2021**, *15*, 5396–5404. [CrossRef]
25. Cai, H.; Wang, Z.; Xie, D.; Zhao, P.; Sun, J.; Qin, D.; Cheng, F. Flexible transparent wood enabled by epoxy resin and ethylene glycol diglycidyl ether. *J. Forestry Res.* **2021**, *32*, 1779–1787. [CrossRef]
26. Wang, K.; Liu, X.; Dong, Y.; Ling, Z.; Cai, Y.; Tian, D.; Fang, Z.; Li, J. Editable shape-memory transparent wood based on epoxy-based dynamic covalent polymer with excellent optical and thermal management for smart building materials. *Cellulose* **2022**, *29*, 7955–7972. [CrossRef]
27. Wu, X.; Kong, Z.; Yao, X.; Gan, J.; Zhan, X.; Wu, Y. Transparent wood with self-cleaning properties for next-generation smart photovoltaic panels. *Appl. Surf. Sci.* **2023**, *613*, 155927. [CrossRef]
28. Zhang, T.; Yang, P.; Li, Y.; Cao, Y.; Zhou, Y.; Chen, M.; Zhu, Z.; Chen, W.; Zhou, X. Flexible transparent sliced veneer for alternating current electroluminescent devices. *ACS Sustain. Chem. Eng.* **2019**, *7*, 11464–11473. [CrossRef]
29. Höglund, M.; Garemark, J.; Nero, M.; Willhammar, T.; Popov, S.; Berglund, L.A. Facile processing of transparent wood nanocomposites with structural color from plasmonic nanoparticles. *Chem. Mater.* **2021**, *33*, 3736–3745. [CrossRef]
30. Yu, Z.; Yao, Y.; Yao, J.; Zhang, L.; Chen, Z.; Gao, Y.; Luo, H. Transparent wood containing Cs × WO_3 nanoparticles for heat-shielding window applications. *J. Mater. Chem. A* **2017**, *5*, 6019–6024. [CrossRef]
31. Qiu, Z.; Xiao, Z.; Gao, L.; Li, J.; Wang, H.; Wang, Y.; Xie, Y. Transparent wood bearing a shielding effect to infrared heat and ultraviolet via incorporation of modified antimony-doped tin oxide nanoparticles. *Compos. Sci. Technol.* **2019**, *172*, 43–48. [CrossRef]
32. Wu, T.; Xu, Y.; Cui, Z.; Li, H.; Wang, K.; Kang, L.; Cai, Y.; Li, J.; Tian, D. Efficient heat shielding and ultraviolet isolating transparent wood via in situ generation of TiO_2 nanoparticles. *ACS Sustain. Chem. Eng.* **2022**, *10*, 15380–15388. [CrossRef]
33. Aldalbahi, A.; El-Naggar, M.E.; Khattab, T.A.; Hossain, M. Preparation of flame-retardant, hydrophobic, ultraviolet protective, and luminescent transparent wood. *Luminescence* **2021**, *36*, 1922–1932. [CrossRef]
34. Rahayu, I.; Prihatini, E.; Ismail, R.; Darmawan, W.; Karlinasari, L.; Laksono, G.D. Fast-growing magnetic wood synthesis by an in-situ method. *Polymers* **2022**, *14*, 2137. [CrossRef]
35. Li, T.; Zhai, Y.; He, S.; Gan, W.; Wei, Z.; Heidarinejad, M.; Dalgo, D.; Mi, R.; Zhao, X.; Song, J.; et al. A radiative cooling structural material. *Science* **2019**, *364*, 760–763. [CrossRef]
36. Xia, Q.; Chen, C.; Li, T.; He, S.; Gao, J.; Wang, X.; Hu, L. Solar-assisted fabrication of large-scale, patternable transparent wood. *Sci. Adv.* **2021**, *7*, eabd7342. [CrossRef]
37. Zhu, M.; Song, J.; Li, T.; Gong, A.; Wang, Y.; Dai, J.; Yao, Y.; Luo, W.; Henderson, D.; Hu, L. Highly anisotropic, highly transparent wood composites. *Adv. Mater.* **2016**, *28*, 5181–5187. [CrossRef]
38. Liu, S.; Tso, C.Y.; Lee, H.H.; Du, Y.W.; Yu, K.M.; Feng, S.-P.; Huang, B. Self-densified optically transparent VO_2 thermochromic wood film for smart windows. *ACS Appl. Mater. Interfaces* **2021**, *13*, 22495–22504. [CrossRef]
39. Zhang, K.; Chu, C.; Li, M.; Li, W.; Li, J.; Guo, X.; Ding, Y. Transparent wood developed by impregnating poplar with epoxy resin assisted by silane coupling agent. *Bioresources* **2023**, *18*, 3598–3607. [CrossRef]